Supplementary Information

Flexible PANI/SWCNT thermoelectric films with ultrahigh electrical conductivity

Ruili Wu [a], Haocheng Yuan [a], Chan Liu [b], Yuan-Hua Lin [b], Xiaoping Yang [a]*, Jin-Le Lan [a]*

[a] State Key Laboratory of Organic-Inorganic Composites, Beijing University of Chemical Technology, Beijing 100029, China

[b] State Key Laboratory of New Ceramics and Fine Processing, School of Materials Science and Engineering, Tsinghua University, Beijing, 100084, P. R. China

*Author to whom correspondence should be addressed. E-mail: lanjl@mail.buct.edu.cn, yangxp@mail.buct.edu.cn

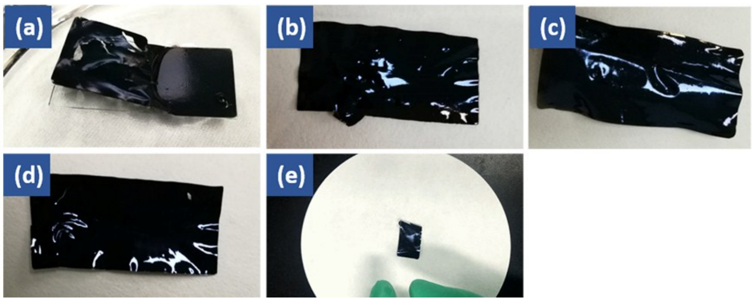

Figure S1. The optical photography of PANI films at different polymerization time, (a) 5h, (b) 6h, (c) 12h, (d) 18h, (e) 24h

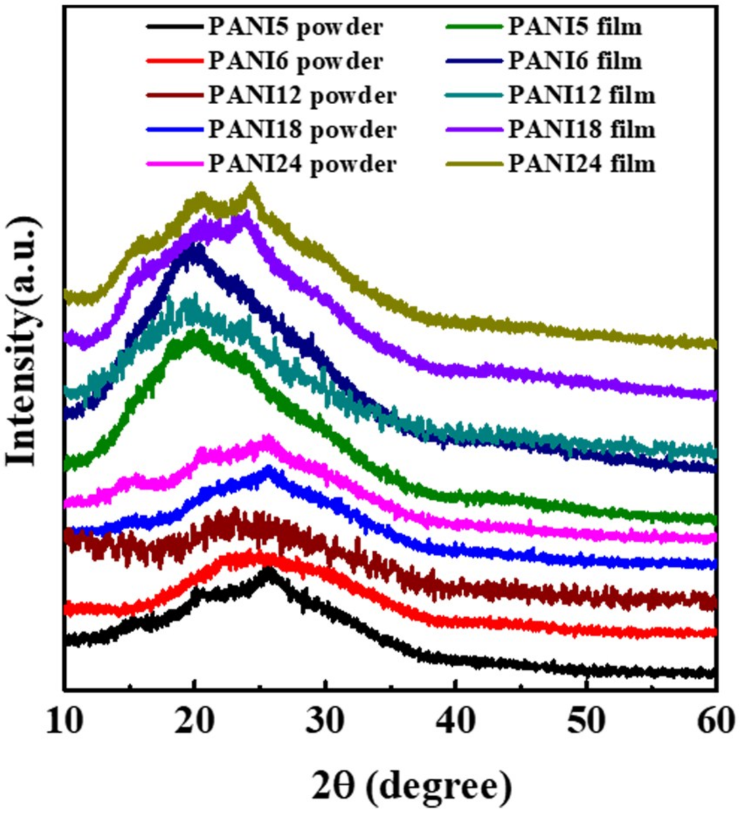

Figure S2. The XRD patterns of PANI with different polymerization time.

Table S1. GPC data of pure PANI films.

PANI	**Mn**	**Mw**	**Mp**	**Mz**	**Mz+1**	**Polydispersity**
0℃，5h	36951	37972	37879	39000	40033	1.03
0℃，6h	21082	34470	31506	50454	66083	1.64
0℃，12h	23700	42568	41498	64386	85408	1.80
0℃，18h	24311	41294	35964	62830	84888	1.70
0℃，24h	19998	50302	43609	98455	157444	2.52
25℃，5h	21880	70572	30909	239594	514314	3.22

Table S2. List of Samples Containing Different Types of PANI and CNT with Various CNT Concentrations

Sample no.	**CNT concentrations （wt %）**	**CNT(mg)**	**PANI(mg)**	**CSA(mg)**
1	0	0	22	28
2	5	1.13	21.50	27.37
3	10	2.33	20.97	26.70
4	30	7.93	18.51	23.56
5	50	15.28	15.28	19.45
6	60	19.88	13.25	16.87
7	70	25.33	10.86	13.82
8	90	39.92	4.44	5.65

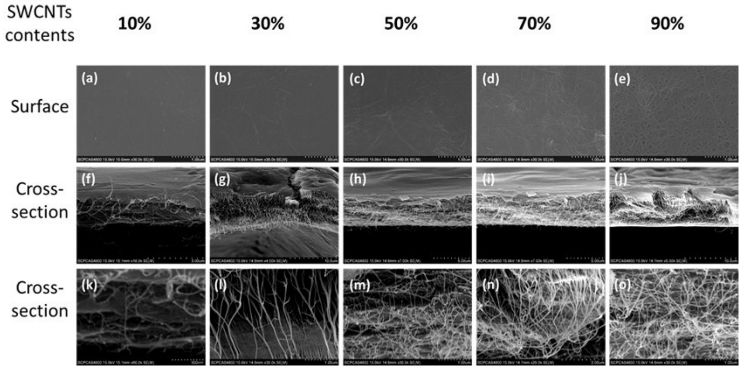

Figure S3. SEM image of PANI/SWCNT with different CNT content.

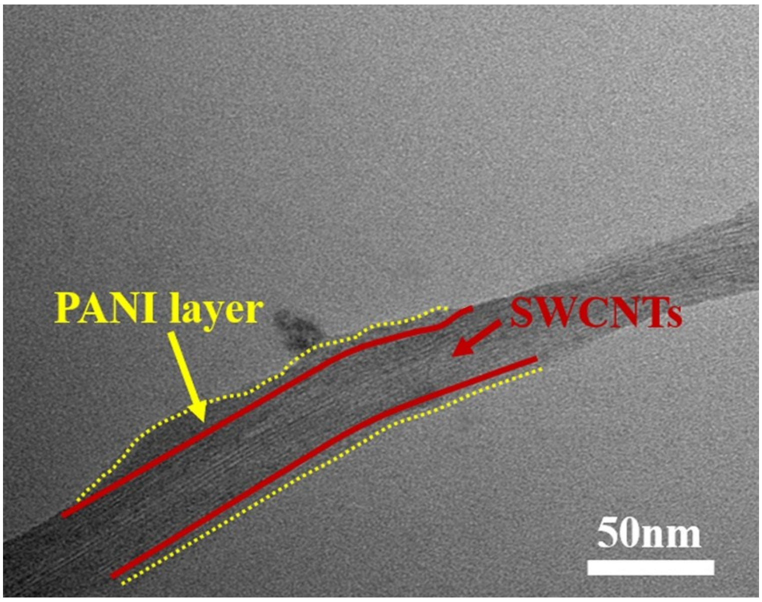

Figure S4. TEM image of the SWCNTs/PANI composite films with 60wt% SWCNTs.

The TEM image of the SWCNTs/PANI composite films was shown in Figure S4. The SWCNTs bundles acted as the backbone of the composites, and a thin PANI layer was closely coated on the surface of the SWCNTs. This observation further proves that the PANI chains wrapped around the outside of the SWCNTs, which can be attributed to the interactions between PANI and SWCNTs.

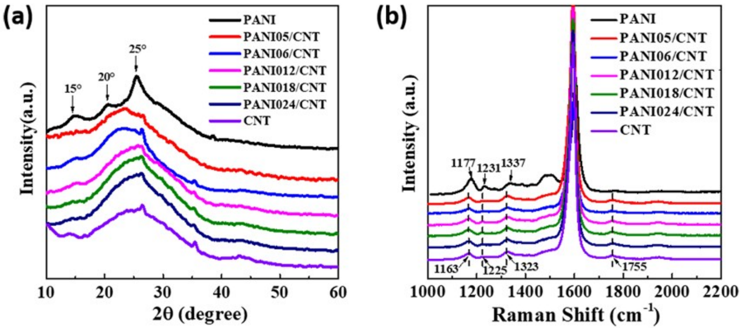

Figure S5. XRD patterns (a) and Raman (b) of SWCNT/PANI with content of different CNT.

Fig. S5(a) presents the XRD patterns of the SWCNTs/PANI composite film with PANI of different polymerization time. The pure SWCNT films exhibits a strong typical diffraction peak at 2θ=26.2°. The pure PANI film shows three diffraction peaks, at 2θ=15°, 20°and 25°, assigning to the repeat unit of the PANI chain, the periodicity perpendicular to the polymer backbone chain, and periodicity parallel to the polymer backbone chain, respectively. The characteristic diffraction peaks of PANI almost disappeared after compounding, indicating that the interaction between PANI and SWCNT occurred, which changed the molecular conformation of PANI and arrangement of PANI molecular chains that changed from the curled state to the stretched state.

Fig. S5(b) is the Raman spectra of pure PANI, SWCNT and their composite film with PANI of different polymerization time. After compounding, some diffraction peaks of PANI near by ~1500 cm^{-1} disappeared, suggesting that there is a strong interaction between PANI and SWCNTs, which changes the structure of PANI. At other characteristic peaks of polyaniline, including 1177 cm^{-1} (C–H bending vibration of the quinoid/benzenoid rings), 1337 cm^{-1} (C–N^{+} vibration of delocalized polaronic structures), obviously shifted to the low frequency in the composite films, indicating that there existed a strong π-π conjugated interactions between PANI and SWCNTs, and the conjugation could enhance the electron delocalization and cause a Raman shift. In addition, it has been reported that the π-π conjugated interactions can induce a conformation of the PANI molecule from a coil-like structure to an extended structure. Therefore, it is believed that there are more ordered PANI molecular structure regions in the PANI/CNTs composite films.

Moreover, the XRD patterns and Raman spectra of the composites are basically same, indicating that PANI with different polymerization time has not so significant effect on the structure of the composites comparing with high content filler. It also explains why its TE performance basically unchanged.

percolation theory：

The electrical conductivity of these polymer composites generally obeys a power law, which usually used in the composite systems:

$$\sigma = \sigma_0 (V - V_c)^t \qquad \text{Eq. (1)}$$

where σ_0 is a proportionality constant related to the effect intrinsic conductivity of CNT in the composite, V is the volume fraction of CNT, V_c is the critical volume fraction of CNT to produce the conductive network, and t is the power law exponent.

the series- and parallel-connected models：

The series- and parallel-connected models between the SWCNTs and PANI can be written as:

$$\sigma_s{}^{-1} = (1 - v_{CNT})\sigma_{PANI}{}^{-1} + v_{CNT}\sigma_{CNT}{}^{-1} \qquad \text{Eq. (2)}$$

$$\sigma_p = (1 - v_{CNT})\sigma_{PANI} + v_{CNT}\sigma_{CNT} \qquad \text{Eq. (3)}$$

$$S_p = \frac{(1 - v_{CNT})\sigma_{PANI}S_{PANI} + v_{CNT}\sigma_{CNT}S_{CNT}}{(1 - v_{CNT})\sigma_{PANI} + v_{CNT}\sigma_{CNT}} \qquad \text{Eq. (4)}$$

Where σ_s, σ_p, v_{CNT} and S_p are the series-connected electrical conductivity of the composite, parallel-connected electrical conductivity of composite, volume fraction of the SWCNT, and the Seebeck coefficient values of the parallel-connected composite